COMMUNICATION

Check for updates

V-shaped donor–acceptor organic emitters. A new approach towards efficient TADF OLED devices†‡

Wojciech Derkowski,§[a] Dharmandra Kumar,§[b] Tomasz Gryber, [iD]§[c] Jakub Wagner,[a] Maja Morawiak,[a] Michał Andrzej Kochman,[c] Adam Kubas, [iD]*[c] Przemysław Data*[b] and Marcin Lindner [iD]*[a]

We report the synthesis and characterization of a series of donor–acceptor TADF emitters with a new architecture, where the donor moiety and the dibenzazepine-based acceptor moiety are separated by a phenylene linker in a V-shaped spatial arrangement. Such spatial separation and electronic decoupling between the donor and the acceptor moieties leads to low singlet-triplet energy gaps and favors efficient exciton up-conversion.

Organic molecules demonstrating the thermally activated delayed fluorescence (TADF)[1] phenomenon can theoretically produce 100% internal quantum efficiency (IQE) giving rise to a new class of emitters for OLED applications. Thanks to small singlet-triplet energy gaps ($\Delta E_{ST} < 0.2$ eV), triplet excitons can be transferred *via* reverse intersystem crossing (rISC)[2] to the singlet excited state.[3] A range of molecular design strategies have been proposed in order to minimize HOMO-LUMO overlap and meet other fundamental prerequisites for TADF emission.[4,5] These often lead to rigid and planar π-electron platforms having on one side fused electron-accepting moieties (A) and on the other side twisted electron-donating units (D). Accordingly, a considerable number of charge-transfer (CT) chromophores based on carbazole decorated benzonitriles,[1]

phenazines,[6] acenaphthenes[7] and their anthracene[8] counterparts, benzene[9,10]/naphthalene[11] monoimides, dibenzophenazines,[12] and numerous other small planar heterocyclic scaffolds[13] have been synthesized to this end over last few years. Importantly, the smaller the ΔE_{ST} that can be reached, the more efficient the rISC kinetics will be. Along this line, the design strategy based on rigid π-electron emitters seems to be approaching its development limits with ΔE_{ST} often between 0.1–0.2 eV. New design strategies are needed in order to obtain systems with near-zero ΔE_{ST} values. A potential solution to this challenge is the use of V-shaped molecules with distant and almost non-communicating D–A units which are here proposed as TADF emitters. Notably, V-shaped but non-conjugated compounds have been solely used as host TADF materials.[14]

Adopting a new design strategy, we recently demonstrated that a nitrogen-doped polycyclic aromatic hydrocarbon (N-PAH) scaffold incorporating dibenzazepine (see Fig. 1) can provide the basis for efficient TADF emitters.[15] We sought to utilise the modular nature of this system, by releasing the structural tension of the concave N-heterotriangulene to achieve a V-shaped topology. The angled benzene ring protruding from the dibenzazepine acceptor core can be functionalized with a set of aromatic amine donors to potentially provide diverted orientations of the HOMO and LUMO. This molecular

[a] *Institute of Organic Chemistry, Polish Academy of Sciences, Kasprzaka 44/52, Warsaw 01-224, Poland. E-mail: marcin.lindner@icho.edu.pl*

[b] *Łódź University of Technology, Department of Chemistry, Stefana Żeromskiego 114, Łódź 90-543, Poland*

[c] *Institute of Physical Chemistry, Polish Academy of Sciences, Kasprzaka 44/52, Warsaw 01-224, Poland*

† This article is dedicated to the memory of Wojciech Derkowski, who sadly passed away unexpectedly during the preparation of this manuscript.

‡ Electronic supplementary information (ESI) available: Experimental procedures for the syntheses of materials, spectroscopic data of new compounds, single crystal X-ray crystallographic data, cyclic voltammogram, thermogravimetric analysis (TGA) profiles, the copies of NMR spectra of new compounds, and theoretical calculation details. CCDC 2216025–2216027. For ESI and crystallographic data in CIF or other electronic format see DOI: https://doi.org/10.1039/d2cc06978d
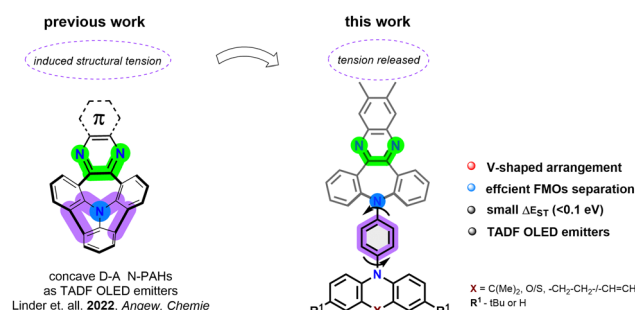
§ These authors contributed equally.

Fig. 1 Detailed molecular strategy present at this work.

architecture also helps prevent aggregation in the solid state, which is a perennial problem with OLED emitters due to aggregation-induced quenching. Using this strategy, we report a new D–A molecular arrangement containing a phenazine fused dibenzazepine (A), linked *via* a benzene spacer, to a variety of aromatic amines (D) to provide V-shaped chromophores which represents a new molecular design paradigm for TADF organic emitters. The demonstrated approach provides an unprecedentedly low ΔE_{ST} thanks to through-space separation of the HOMO–LUMO levels, leading to yellow TADF OLED emitters with appreciable EQE performance with highest value found for **4c** of up to 13.6%.

The title compounds **4a–d** were assembled within four scalable synthetic steps as depicted in Fig. 2a. The synthesis started from the oxidation of commercially available carbamazepine[16] followed by the acid-catalyzed formation of phenazine.[17] Subsequently, a sequence of (chemoselective) Buchwald-Hartwig aminations[18] were performed to first yield intermediate **3** with the installed phenyl bridge and then the set of four desired dyes **4a–d** with D-π-A electronic structures.

The non-planar V-shaped conformation within the set of obtained molecules was unambiguously confirmed by X-ray crystallography of **4a,b** and **4d** (Fig. 2b). Analysis of their structures obtained from single crystal diffraction showed that the angle between the planes of segments, namely, dibenzazepine and benzene bridge donors, was found to range from 110.6°/110.5° (**4a/b**) to 112.9° (**4d**), consistent with our anticipated topology. Interestingly, torsion angles between the benzene and D units are not quite so uniform (85.9°; 90.1°; 85.6° for **4a,b** and **4d**, respectively), which results in a different packing behaviour of emitters in the crystal lattice (for detailed intermolecular interplay see Fig. S11, ESI‡).

The photophysical properties of compounds **4a–d** were characterized with a combination of spectroscopic and computational methods. For the sake of brevity, the detailed description of the calculations is relegated to the ESI.‡ Here, we report only the main results. The photoabsorption and steady-state fluorescence spectra of compounds **4a–d** in dilute organic solutions ($c = 1.0 \times 10^{-5}$ mol L^{-1}) are shown in Fig. S6 (ESI‡). All four compounds show a prominent absorption band in the range of approximately 380–420 nm. According to our electronic structure calculations, in compounds **4a**, **4b**, and **4d**, this absorption band originates mainly from a transition into a $^1\pi\pi^*$-type excited state that is localized on the acceptor moiety (A). In the case of compound **4c**, there is also another excited state that makes a significant contribution to light absorption in this range, namely a $^1\pi\pi^*$-type state localized on the donor moiety (D). Furthermore, the calculations also predict that all four compounds possess donor-to-acceptor intramolecular charge transfer (D → A ICT) states that lie close in energy to the low-lying bright $^1\pi\pi^*$-type states. Transitions from the ground state into the D → A ICT states, however, have negligibly low oscillator strengths, and as such, these states do not make a meaningful contribution to light absorption. Accordingly, in the analysis of fluorescence spectra (see below), we assumed that the fluorescence emission of each compound originates entirely from the lowest $^1\pi\pi^*$-type state.

Moving on to the steady-state fluorescence emission spectra, it can be seen that each of the four compounds exhibit a single fluorescence band which is fairly insensitive to the solvent polarity. Low photoluminescence quantum efficiencies (PLQY), up to 29% for the phenoxazine derivative **4c** in THF (Fig. S6, ESI‡), are also observed. The fact that compounds **4a–d** do not exhibit significant solvatofluorochromism indicates that their fluorescence emission originates from nonpolar excited states. More specifically, calculations suggest that fluorescence emission occurs from the low-lying $^1\pi\pi^*$-type state that is localized on the acceptor moiety (A). Better emissive behaviour is observed in the solid state, where the compounds were investigated in polymer Zeonex® 480r (cyclo olefin polymer) and CBP (4,4′-bis(*N*-carbazolyl)-1,1′-biphenyl) hosts (Fig. S7, ESI‡). Firstly, there is a visible impact of the host on the emission position, where the emission in the CBP host is lower in energy and has increased PLQY in comparison to the respective solutions (Table 1 and Fig. S6, ESI‡). Secondly, the emission in the OLED host CBP when compared to polymer matrix Zeonex, is red-shifted moderately by ∼20 nm for **4a** and **4c** and especially for **4b** (∼40 nm), which suggests a higher contribution of the ^{1}CT state (Fig. S7, ESI‡). The opposite happens for **4d** which exibits a hypsochromic emission shift on moving from Zeonex to CBP. Time-resolved photoluminescence analysis revealed the processes involved in the light generation (Fig. 3 for CBP and Fig. S8 for Zeonex, ESI‡). At first glance, the behaviour of the compounds **4a–d** looks classical, but there are several deviations to the expected behavior. If we look at the compounds based on carbazole (**4a**) and phenoxazine (**4c**), both behave in similar way in both matrices fluorescing from S$_1$ charge transfer states in a very short ns time regime at both 10 K and 300 K (Fig. 3a,e and Fig. S8a,e, ESI‡). The impact of the temperature is observed only after very long
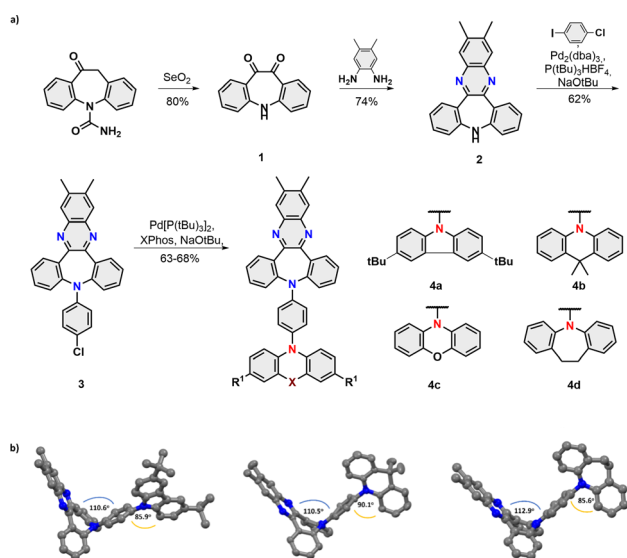

Fig. 2 (a) Synthetic route towards title compounds **4a–d**; (b) Single X-ray structure of the dyes **4a,b, and d**.

Table 1 Summary of the general photophysical properties of compounds **4a–d**
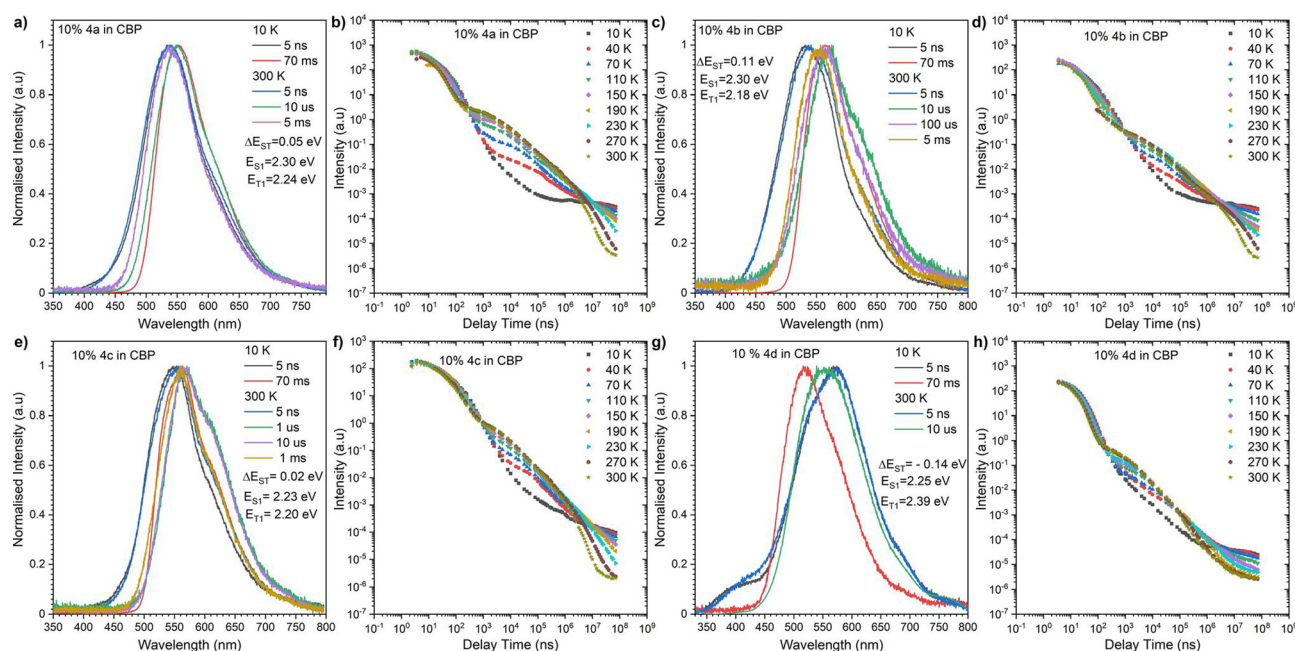
Compound	$\lambda_{em}{}^a$, nm	Host	PLQY^b, %	DF/ PF^c	$S_1{}^d$ eV	$T_1{}^d$ eV	$\Delta E_{ST}{}^e$, eV
4a	513	Zeonex	12.1	32.36	2.43	2.43	0.00
4a	537	CBP	25.6	4.57	2.30	2.25	0.05
4b	504	Zeonex	6.6	17.00	2.46	2.53	−0.07
4b	543	CBP	23.2	2.02	2.31	2.19	0.12
4c	535	Zeonex	14.4	10.52	2.35	2.35	0.00
4c	556	CBP	34	1.98	2.24	2.21	0.03
4d	590	Zeonex	2.6	0.30	2.10	2.33	−0.23
4d	571	CBP	10.5	0.56	2.25	2.39	−0.14

^{a} Photoluminescence maximum. ^{b} Photoluminescence quantum yield. ^{c} Delayed fluorescence (DF) to prompt fluorescence (PF) ratio in the host. ^{d} Singlet and triplet energy in host. Error $\pm$ 0.03 eV. ^{e} Singlet-triplet energy splitting in Zeonex. Error $\pm$ 0.05 eV.

delay times (ms scale), where at 10 K we observe a T_1 localized emission in the form of phosphorescence (Fig. 3a,e and Fig. S8a,e, ESI‡). As temperatue is increased, the phosphorescence emission dissapears and again emission from the S_1 state is observed for which the emission intensity continues to rise with increasing temperature which is a direct observation of the Delayed Fluorescence emission with Thermally Activated (TADF) process (Fig. 3a,b,e,f and Fig. S8a,b,e,f, ESI‡). Together with the ΔE_{ST} gap being close to 0, we would expect a sharp increase in the emission efficiency. Looking at Table 1 we see the PLQY of compounds **4a** and **4c** are moderate, 12.1% **4a** and 14.4% in Zeonex, and 25.6% and 34% in CBP, however, these are measured in air so there is no triplet harvesting. If we take into consideration the DF/PF values, to compare the overall intensity of the Fluorescence and Delayed Fluorescence processes, we could assume, after oxygen removal we should have

maximal harvesting of the triplet state resulting in an increase of the overall emission efficiency (Table 1). So even with the theoretically low PLQY of the compounds, the actuall efficiency would be significantly boosted by the TADF process. More interesting behavior is observed for compounds **4b** and **4d**. 9,10-Dihydro-9,9-dimethylacridine (DMAC) derivatives usually present strong TADF properties, which is also the case for **4b** but in the Zeoenex matrix, a small S–T gap inversion is observed (based on energy of the emission peaks). Generally, it could be assumed that this could be caused by overlap of a couple of emission states and the actuall ΔE_{ST} is around 0 eV (Fig. S8c, ESI‡). Nevertheless, a strong S–T gap inversion is observed for compound **4d**, which could also prove inversion in **4b** possible as well (Fig. 3g and Fig. S8g, ESI‡). The compound **4d**, based on an iminodibenzyl donor, behaves in unusual way, where the phosphorescence emission from the triplet state lies at a higher energy in compared to the lowest singlet state (fluorescence) resulting in a negative S–T gap. Morover, we observe thermally activated delayed fluorescence emission in both Zeonex and CBP matrices (Fig. S8g, ESI‡ and Fig. 3g), which together with a negative S–T gap should result in a faster rISC process and decrease the delayed emission lifetime. Such behaviour is actually observed, where for **4d** the delayed fluorescence emission lifetime is one order magnitude faster than for the other compounds (Fig. 3g and Table 1 and Fig. S3, ESI‡) at around 2.6 µs which is very important for OLED applications. This suggests that the whole excited state will participate in the OLED emission, as usually long-lived excited states are quenched by polarons.

As the final stage of the investigation, OLED devices based on **4a–4d** were prepared and analysed (Fig. 4). To prepare the

Fig. 3 Time-Resolved Spectra of compounds **4a–d** in CBP matrix (a, c, e and g), the energies correspond to the maximum emission peaks. Intensity vs delay time measurement decays (b, d, f and h).
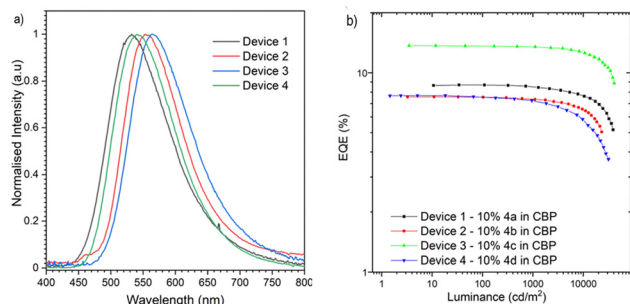
Fig. 4 The characteristics of the OLED devices based on emitters **4a–d**. (a) Electroluminescence spectra. (b) EQE–luminance characteristics.

proper structure the ionization potenatial (IP) and electron affinity (EA) of the compounds are needed. The electrochemical behavior of **4a–d** in dichloromethane was investigated with cyclic voltammetry (CV) (Fig. S9, ESI‡). All compounds exhibited reversible oxidation process with the highest IP for the carbazol derivative (**4a**) at around −5.53 eV. The reduction process for all compounds is irreversible but no additional products were formed sugesting rather low stability of the carboanion. The electron affinity of the compounds is rather similar at around −3.09 eV suggesting lack of impact of the donor and good separation of the donor and acceptor and no conjugation (Fig. S9, ESI‡). With the knowledge of the IP/EA energies, the following two OLED structures were deposited using high-vacuum thermal evaporators, ITO/NPB (30 nm)/TAPC (10 nm)/10% **4a–4d** in CBP (25 nm)/TPBi (50 nm)/LiF (1 nm)/Al (100 nm). The fabricated OLED devices and photophysical results were compared in order to evaluate emissive pathways that boost the efficiency properties. In all of the OLED devices we observed emission from the S_1 state with the external quantum efficiency (EQE) above the theoretical maximum for only fluorescence emitters (>5%) (Fig. 4). The electroluminescence spectra matched the delayed emission obtained in the photophysical analysis of synthesized compounds in CBP matrix and with the ΔE_{ST} gap close to 0, proving that the emission is associated with the TADF process. The highest external quantum efficiency (EQE) of the OLEDs was obtained with the phenoxazine based derivative **4c** (13.6%), whereas the device with the inverted S–T gap **4d** showed a lower EQE of 7.7% (Fig. 4b and Fig. S12‡). These EQE values may not be as high as other reported TADF OLED devices, however, the efficiency is one of the highest for negative ΔE_{ST} emitters. Moreover, if we look to the luminance, the highest value was observed for the carbazole derivative (above 38 000 cd m^{-2}), nevertheless for the rest of the compounds the values are above 30 000 cd m^{-2} which is quite high, and prove proper device structure and efficient recombination. The lower efficiency of the device based on compound **4d** is associated with non-emissive recombination from the triplet state, and the DF/PF value is rather low which suggests that at least in the photo-excited process, the energy from the triplet excited state is lost. Similar behaviour was observed in our previous study,[19] however, in that case we didn't observe a negative ΔE_{ST} gap. In

our current study, compound **4d** exhibits better performance suggesting the continued study of such derivaties could bring promising results in the future.

In summary, we have presented a new class of rationally designed organic emitters with a V-shaped geometry. Features of these chromophores significantly enhance their FMO overlap which translates to very small ΔE_{ST} values (<0.1 eV). Beyond appreciable photoluminescence quantum yields (PLQYs) of up to 36% for the phenoxazine containing emitter, the proposed arrangement contributes significantly to efficient TADF emission. Building on this, OLED devices were fabricated and the best-performing compound in the series, bearing an electron-rich phenoxazine group, displayed a very high efficiency of 13.6%. This work provides a new avenue for emissive V-shaped organic materials in the future. Moreover, increasing a strength of electron-accepting group is supposed to contribute to elevated PLQY values which is currently under studies.

Conflicts of interest

There are no conflicts to declare.

Notes and references

1 K. Goushi, K. Yoshida, K. Sato and C. Adachi, *Nat. Photonics*, 2012, **6**, 253–258.
2 F. B. Dias, K. N. Bourdakos, V. Jankus, K. C. Moss, K. T. Kamtekar, V. Bhalla, J. Santos, M. R. Bryce and A. P. Monkman, *Adv. Mater.*, 2013, **25**, 3707–3714.
3 P. Data and Y. Takeda, *Chem. – Asian J.*, 2019, **14**, 1613–1636.
4 J.-F. Cheng, Z.-H. Pan, K. Zhang, Y. Zhao, C.-K. Wang, L. Ding, M.-K. Fung and J. Fan, *Chem. Eng. J.*, 2022, **430**, 132744.
5 Z. Feng, S. Yang, F. Kong, Y. Qu, X. Meng, D. Yu, D. Zhou, Z. Jiang and L. Liao, *Adv. Funct. Mater.*, 2022, 2209708.
6 J. Chen, W. Tao, W. Chen, Y. Xiao, K. Wang, C. Cao, J. Yu, S. Li, F. Geng, C. Adachi, C. Lee and X. Zhang, *Angew. Chem., Int. Ed.*, 2019, **58**, 14660–14665.
7 U. Balijapalli, Y. Lee, B. S. B. Karunathilaka, G. Tumen-Ulzii, M. Auffray, Y. Tsuchiya, H. Nakanotani and C. Adachi, *Angew. Chem., Int. Ed.*, 2021, **60**, 19364–19373.
8 Y. Yu, Y. Hu, S. Yang, W. Luo, Y. Yuan, C. Peng, J. Liu, A. Khan, Z. Jiang and L. Liao, *Angew. Chem., Int. Ed.*, 2020, **59**, 21578–21584.
9 M. Li, Y. Liu, R. Duan, X. Wei, Y. Yi, Y. Wang and C.-F. Chen, *Angew. Chem., Int. Ed.*, 2017, **56**, 8818–8822.
10 Z. Huang, B. Lei, D. Yang, D. Ma, Z. Bin and J. You, *Angew. Chem., Int. Ed.*, 2022, **61**, e202213157.
11 W. Zeng, H.-Y. Lai, W.-K. Lee, M. Jiao, Y.-J. Shiu, C. Zhong, S. Gong, T. Zhou, G. Xie, M. Sarma, K.-T. Wong, C.-C. Wu and C. Yang, *Adv. Mater.*, 2018, **30**, 1704961.
12 P. Data, P. Pander, M. Okazaki, Y. Takeda, S. Minakata and A. P. Monkman, *Angew. Chem., Int. Ed.*, 2016, **55**, 5739–5744.
13 D. Sun, R. Saxena, X. Fan, S. Athanasopoulos, E. Duda, M. Zhang, S. Bagnich, X. Zhang, E. Zysman-Colman and A. Köhler, *Adv. Sci.*, 2022, **9**, 2201470.
14 D. W. Lee, J. Hwang, H. J. Kim, H. Lee, J. M. Ha, H. Y. Woo, S. Park, M. J. Cho and D. H. Choi, *ACS Appl. Mater. Interfaces*, 2021, **13**, 49076–49084.
15 J. Wagner, P. Zimmermann Crocomo, M. A. Kochman, A. Kubas, P. Data and M. Lindner, *Angew. Chem., Int. Ed.*, 2022, **61**, e202202232.
16 M. Parravicini, L. Vaghi, G. Cravotto, N. Masciocchi, A. Maspero, G. Palmisano and A. Penoni, *Arkivoc*, 2014, 72.
17 C.-T. Chen, J.-S. Lin, M. V. R. K. Moturu, Y.-W. Lin, W. Yi, Y.-T. Tao and C.-H. Chien, *Chem. Commun.*, 2005, 3980–3982.
18 P. Ruiz-Castillo and S. L. Buchwald, *Chem. Rev.*, 2016, **116**, 12564–12649.
19 P. Zimmermann Crocomo, T. Kaihara, S. Kawaguchi., P. Stachelek, S. Minakata, P. Silva, P. Data and Y. Takeda, *Chem. – Eur. J.*, 2021, **27**, 13390–13398.